Agricultural Systems 196 (2022) 103340

Contents lists available at ScienceDirect

Agricultural Systems

journal homepage: www.elsevier.com/locate/agsy

Assessing climate vulnerability of historical wheat yield in south-eastern Australia's wheat belt

Siyi Li[a,b,c], Bin Wang[c,*], Puyu Feng[e], De Li Liu[c,d,*], Linchao Li[a], Lijie Shi[b,c], Qiang Yu[a,b,f,**]

[a] State Key Laboratory of Soil Erosion and Dryland Farming on the Loess Plateau, Institute of Soil and Water Conservation, Northwest A&F University, Yangling, Shaanxi 712100, China
[b] School of Life Sciences, Faculty of Science, University of Technology Sydney, PO Box 123, Broadway, Sydney, NSW 2007, Australia
[c] NSW Department of Primary Industries, Wagga Wagga Agricultural Institute, Wagga Wagga, NSW 2650, Australia
[d] Climate Change Research Centre, University of New South Wales, Sydney, NSW 2052, Australia
[e] College of Land Science and Technology, China Agricultural University, Beijing, 100193, China
[f] Key Laboratory of Water Cycle and Related Land Surface Processes, Institute of Geographic Sciences and Natural Resources Research, Chinese Academy of Sciences, Beijing 100101, China

HIGHLIGHTS

- A modified indicator-based method was developed to assess wheat yield vulnerability.
- Machine learning was used to obtain weights of climate indices when calculating exposure.
- Historical vulnerability of wheat yield decreased as the improved adaptive capacity.
- The most vulnerable areas were the north-western parts of the wheat belt.
- This vulnerability assessment method can be applied to other regions with long-term data of crop yield and climate.

GRAPHICAL ABSTRACT

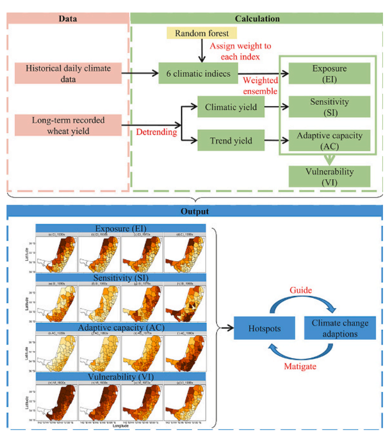

ARTICLE INFO

Editor: Mark van Wijk

Keywords:
Climate vulnerability
Wheat yield
Exposure index
Adaptive capacity

ABSTRACT

CONTEXT: Agricultural vulnerability assessment is a comprehensive and powerful analytical tool to locate hotspots with states of susceptibility to harm and powerlessness of agricultural system. It plays an important role in guiding policy makers to plan and implement adaptation practices to mitigate potential climate risks to crop. However, due to the diversity in the methodology of vulnerability assessment, there are still knowledge gaps in assessing and comparing crop vulnerability to climate in different regions of the world, including Australia.
OBJECTIVE: Our main objectives were to: (1) present a vulnerability analytical method for wheat yield, which can be applied to different areas where long-term crop yield and climate data are available. (2) quantify temporal

* Corresponding authors at: NSW Department of Primary Industries, Wagga Wagga Agricultural Institute, Wagga Wagga, NSW 2650, Australia.
** Corresponding author at: State Key Laboratory of Soil Erosion and Dryland Farming on the Loess Plateau, Institute of Soil and Water Conservation, Northwest A&F University, Yangling, Shaanxi 712100, China.
E-mail addresses: bin.a.wang@dpi.nsw.gov.au (B. Wang), de.li.liu@dpi.nsw.gov.au (D.L. Liu), yuq@nwafu.edu.cn (Q. Yu).

https://doi.org/10.1016/j.agsy.2021.103340
Received 25 June 2021; Received in revised form 29 September 2021; Accepted 29 November 2021
Available online 7 December 2021

Wheat belt
South-eastern Australia

changes of the vulnerability of wheat yield to historical climate. (3) identify the most vulnerable region in study area to provide guidance for climate mitigation.

METHODS: Our study developed an indicator-based method using exposure, sensitivity, and adaptive capacity to assess the vulnerability of crop yield. We used the long-term recorded wheat yield data, combining with comprehensive exposure index to assess climate vulnerability of historical yield with a case study area of south-eastern Australia's wheat belt.

RESULTS AND CONCLUSIONS: The results showed that from the 1930s to the 1990s, both climate exposure and sensitivity had large inter-annual variations with no significant trends detected. However, adaptive capacity increased by 34% from 1930s to 1950s, 54% from 1950s to 1970s, and 54% from 1970s to 1990s. By contrast, climate vulnerability across the wheat belt decreased by 13% from 1930s to 1950s, 15% from 1950s to 1970s, and 33% from 1970s to 1990s. This is mainly due to increased adaptive capacity with the improvement of agronomic management practices, technological and socio-economic progress. We identified the areas with the highest vulnerability were in the northwestern parts of wheat belt while the least vulnerable areas located in the southeast.

SIGNIFICANCE: We expect that these identified vulnerable hotspots can be used by different landholders to allocate natural resources and policymakers to plan the priority mitigation to adapt to climate change in the local scale. Moreover, the method of vulnerability assessment used in this study can be applied to other regions around the world where long-term crop yield and climate data are available.

1. Introduction

Climate change has great impacts on agro-ecological environments, leading to significant changes in crop productivity (Yang et al., 2015; Kurukulasuriya and Mendelsohn, 2008). For example, from 1980 to 2008, global wheat yield has decreased by 1.4%–2.0% per decade due to the warming climate (Lobell et al., 2011). The cycles of droughts and flooding associated with the El Niño phenomenon have explained between 15% and 35% of global yield variability (Howden et al., 2007). The unstable crop yield may increase difficulty of maintaining global food security with the growing world population (Ray et al., 2013).

Numerous studies have used vulnerability assessment to assess the impacts of climate change on agricultural crop yield (Lal et al., 1998; Li et al., 2014; Sonkar et al., 2019). Climate vulnerability of crop yield can be defined as the "degree that crop is susceptible to, or unable to cope with, adverse effects of climate change, including climate variability and extremes" (McCarthy et al., 2001; IPCC, 2007; IPCC, 2012). It is a function of the sensitivity, exposure, and adaptive capacity of crop yield to climate change. Vulnerability assessment for crop yield can not only assess the impact of climate change and socio-economic development on crop productivity, but also analyze the effectiveness and adaptability of different agronomic adaptations (Kamali et al., 2018b; Wang et al., 2020). It is a powerful analytical tool to locate hotspots with states of susceptibility to harm and powerlessness (Adger, 2006), which can guide policy makers to plan and implement adaptation practices to slow down or eliminate potential harm to cropping systems. It plays an important role in promoting crop productivity to actively adapt to climate change, keeping stable and continuous growth of crop yield, and ensuring food security (Senapati et al., 2021; Kamali et al., 2018a).

In recent years, different methods, mainly including the process-based crop growth model (Yue et al., 2015; Wang et al., 2020; Li et al., 2015) and the indicator-based method (Sendhil et al., 2018; Neset et al., 2019; Gbetibouo et al., 2010), were developed to evaluate the vulnerability of crop yield to historical and future climate change around the world. The crop growth model is driven by different climate data and can simulate the response of yield to climate change, which is used to assess the vulnerability under some specific events, such as water stress (Li et al., 2015; Kamali et al., 2018a) and heat stress (Semenov and Shewry, 2011). However, this method is not comprehensive enough, because it usually separately assesses crop vulnerability caused by single limiting factor, rainfall (Li et al., 2015; Yue et al., 2015) or temperature (Semenov and Shewry, 2011). In general, these limiting factors of climate on crop yield can occur at the same time (Sun et al., 2019), and often interact on each other (Zaitchik et al., 2006; Bandyopadhyay et al., 2016). In addition, the crop growth model has a less accurate performance in simulating the impacts of extreme weather events, and the model cannot consider the impacts of pests and diseases, socio-economic, and technological progress (Semenov and Shewry, 2011; Wang et al., 2020). On the contrary, the indicator-based method can evaluate the vulnerability of a system from multiple dimensions (Pandey et al., 2017; Ahmadalipour and Moradkhani, 2018). Indicators related to the system are selected from multiple sectors (climate, social economy, land use, resources, and infrastructure, etc.) to obtain relatively comprehensive vulnerability results. Additionally, the indicator-based method has strong customization, as it can select relevant indicators according to different research objects and objectives. Therefore, this method is a better choice for a relatively comprehensive assessment of crop yield vulnerability. Nonetheless, this method also has shortcomings. It is limited in producing a unified set of indicators due to the different backgrounds of social economy and management measures in different regions. Some researchers have reported that this method is unfavourable for vulnerability assessment and comparison on a large scale (Hinkel, 2011). We intended to create the possibility of assessing and comparing the vulnerability on a large scale. Therefore, we used a modified indicator-based method to assess the climate vulnerability of agricultural crop yields based on the data of climate and yields.

Australia is a major food producer and exporter, and its wheat, barley, and canola have made up 10%–40% of the world's export trade (AEGIC, 2021). Australia's grain production is crucial to the national economy, and makes an important contribution to the global food security and the stability of agricultural product prices. However, the crop yield in Australia varied greatly from year to year, and even showed a stagnant trend in the past 30 years (Hochman et al., 2017). For example, during 1989 to 2020, the wheat yield ranged from 0.92 to 2.61 t/ha (ABARES, 2021). This disturbing trend of yield was largely explained by climate variability. Climate variability resulted in 43% of the total wheat yield variation in Australia from 1979 to 2008 (Ray et al., 2015). Therefore, it is necessary to assess the climate vulnerability in agricultural crop yield to identify those vulnerable hotspots in Australia. This knowledge would allow the development of more targeted policy and management implementation to mitigate current climatic challenges and reduce future risk (Ericksen et al., 2011; Abson et al., 2012).

Few studies have assessed the climate vulnerability of crop yield in Australia (Bryan et al., 2015; Huai, 2016; Wang et al., 2020). Most of these studies used crop simulation models to assess vulnerability under climate change. For example, Wang et al. (2020) assessed the biophysical vulnerability of wheat to future climate change using the yield simulated from APSIM-Wheat model under different scenarios. However, they did not consider the impact of socio-economic factors and advances in agronomic managements on adaptive capacity. Similarly, other researchers assessed the vulnerability based on crop yield, and also analyzed the correlation between vulnerability and different capital indicators (e.g. social, human, physical, natural, and financial capital) (Bryan et al., 2015; Huai, 2016). However, these studies used a single climate index (relative standardized precipitation and evapotranspiration index or maximum annual temperature) to characterize exposure. They did not fully take into account the impacts of extreme climate events associated with both temperature and rainfall. Thus, there are still knowledge gaps on how vulnerable Australia's wheat production is in response to climate change.

Here, our study developed a modified indicator-based method based on exposure, sensitivity, and adaptive capacity to assess the vulnerability of historical wheat yield to climate change in south-eastern Australia. Our main objectives were to: (1) present a vulnerability analytical method for wheat yield, which can be applied to different areas where long-term crop yield and climate data are available. (2) quantify temporal changes of the vulnerability of wheat yield to historical climate. (3) identify the most vulnerable region in the study area to provide guidance for climate change mitigation.

2. Materials and methods

2.1. Study area and data sources

Our study area is located in the state of New South Wales (NSW) wheat belt in the southeast of Australia and covered by 66 shires (Table 1), which is a major wheat producing area in Australia. The wheat production in this area accounts for 27% of total national wheat production and 26% of total national wheat planted area (ABARES, 2021). Over the past three decades (1989–2020), annual wheat production in NSW wheat belt ranged between 3423 kt and 13,110 kt, and the harvested area in NSW varied from 2123 to 3800 kha (ABARES, 2021). Overall, yield per hectare varied greatly from 1.61 to 3.45 t/ha. The large inter-annual fluctuation in wheat yield can be largely attributed to climate variability and change (Wang et al., 2015).

There are large variations in the climate and topography across the wheat belt. During the wheat growing season (April to November), average rainfall ranges from 159 mm in the southwest to 677 mm in the northeast of the NSW wheat belt (Wang et al., 2017). Wheat growing season temperature gradually decreases from 14 °C in the north to 12 °C in the south (Feng et al., 2018). The terrain of eastern parts of study area is hills with an altitude of over 500 m. The topography of the western and central region of the wheat belt is mainly occupied by plains. According to climate and topography, the wheat belt was divided into three sub-regions: (I) northern plains (12 shires), (II) southern plains (33 shires), and (III) eastern slopes (21 shires) (Fig. 1).

Wheat yields of 66 shires in the NSW wheat belt were collected from Fitzsimmons (2001). Historical daily climate data (rainfall, solar radiation, evapotranspiration, maximum, and minimum temperature) for 940 weather stations in the study area were obtained from SILO patched point dataset (Jeffrey et al., 2001).

2.2. Vulnerability assessment framework

We selected the wheat yield and different climate indices in the NSW wheat belt to conduct a case study. We systematically assessed the spatio-temporal change of exposure (*EI*), sensitivity (*SI*), adaptive capacity (*AC*), and vulnerability (*VI*) of 66 shires in 1924–1998. Sensitivity is the response of the crop production system to climate change, including both beneficial and harmful effects. Exposure indicates the extent of change mainly in climate (IPCC, 2012). Adaptive capacity is the ability or potential of the crop production system to respond successfully to climate and includes adjustments in behaviors, resources, and technologies (Watson et al., 1996; Watson et al., 1997). Historical

Table 1
Time period of wheat yield data in 66 selected shires in the NSW wheat belt.

Region	ID	Shire	Period	Region	ID	Shire	Period
I	1	Walgett	1966–2000	II	34	Wagga wagga	1922–2000
	2	Moree Plains	1922–2000		35	Junee	1922–2000
	3	Yallaroi	1922–2000		36	Cootamundra	1922–2000
	4	Bingara	1922–1996		37	Lockhart	1922–2000
	5	Narrabri	1922–2000		38	Urana	1922–2000
	6	Coonamble	1922–2000		39	Jerilderie	1922–2000
	7	Warren	1958–2000		40	Conargo	1922–2000
	8	Bogan	1958–2000		41	Windouran	1922–1996
	9	Gilgandra	1922–2000		42	Culcairn	1922–2000
	10	Coonabarabbran	1922–2000		43	Wakool	1922–2000
	11	Coolah	1922–2000		44	Murray	1922–2000
	12	Gunnedah	1922–2000		45	Berrigan	1922–2000
II	13	Lachlan	1922–2000		46	Corowa	1922–2000
	14	Narromine	1922–2000	III	47	Inverell	1922–2000
	15	Dubbo	1922–2000		48	Barraba	1922–1996
	16	Wellington	1922–2000		49	Manilla	1922–1996
	17	Cabonne	1922–2000		50	Parry	1922–2000
	18	Parkes	1922–2000		51	Nundle	1922–1996
	19	Forbes	1922–2000		52	Quirindi	1922–2000
	20	Carrathool	1922–2000		53	Murrurundi	1922–2000
	21	Bland	1922–2000		54	Scone	1922–1996
	22	Weddin	1922–2000		55	Merriwa	1922–2000
	23	Cowra	1922–2000		56	Muswellbrook	1922–1996
	24	Young	1922–2000		57	Rylstone	1922–1996
	25	Temora	1922–2000		58	Mudgee	1922–1996
	26	Coolamon	1922–2000		59	Evans	1922–1996
	27	Narrandera	1922–2000		60	Blayney	1922–1996
	28	Leeton	1927–2000		61	Boorowa	1922–2000
	29	Griffith	1927–2000		62	Yass	1922–1996
	30	Wentworth	1922–2000		63	Harden	1922–2000
	31	Balranald	1960–2000		64	Gundagai	1922–1996
	32	Hay	1961–2000		65	Holbrook	1922–1996
	33	Murrumbidgee	1922–2000		66	Hume	1922–2000

Region I: 12 shires, northern NSW wheat belt; Region II: 33 shires, southern NSW wheat belt; Region III: 21 shires, eastern NSW wheat belt. ID number is the shire number in Fig. 1.

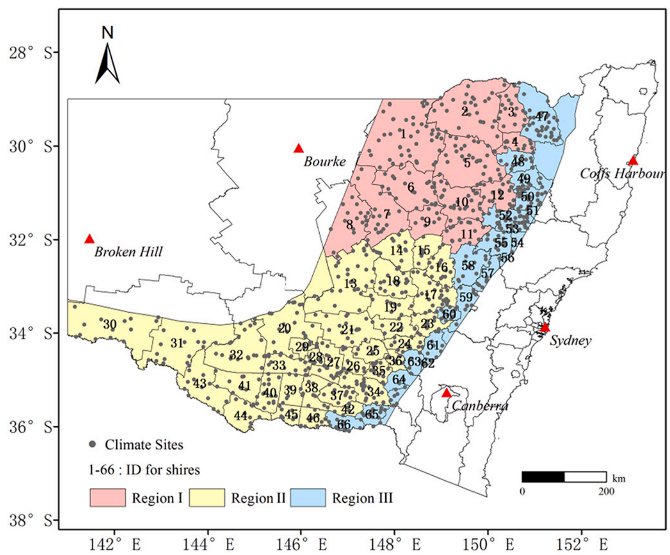

Fig. 1. The distribution of 66 shires and 940 climate stations in three sub-regions in the NSW wheat belt. 1–66 represents the ID of the 66 selected shires in Table 1.

observed crop yield usually reflects the influence of climate-related and non-climate-related factors on cropping system (Eq. (1)). Climatic factors are the main reasons for wheat yield fluctuation. Non-climatic factors are the main driving forces of yield increase, including management practices (breeding, fertilization, and pesticide application), socio-economic, and technology progress, etc.

$$Y = Y_c + Y_t + e \tag{1}$$

where Y is the statistical crop yield (kg/ha); Y_c (kg/ha) is the climatic yield, which is mainly affected by climate variability; Y_t (kg/ha) is the non-climatic yield, which mainly represents the role of agricultural managements; and e is the yield composition influenced by other random factors, which can be ignored (Dong et al., 2018).

We used a commonly-used detrending approach, namely 5-year center moving average model (CMA, Eqs. (2)–(3)) (Lu et al., 2017), to separate wheat yield into climatic yield (Y_{cCMA}) to express the sensitivity (climatic yield is negatively related to the sensitivity, thus we use Eq. (5) to express), and non-climatic yield (Y_{tCMA}) to represent the adaptive capacity of wheat yield to historical climate (Eq. (6)) (Dong et al., 2015). Exposure was calculated by the sum of six weighted climatic indices in Table 2 (Eq. (8)). Finally, the historical vulnerability was calculated by adding *EI* and *SI* then subtracting *AC* (Eq. (9)) (Wang et al., 2020).

The CMA method regarded the crop yield series for 5 consecutive years as a changing linear function, which reflected the historical trend of the yield series as a whole. The average value simulated by sliding linear regression at each year point was the value of the trend at that year. They were calculated as:

$$mY_i = \sum_{j=-2}^{2} \frac{1}{5} Y_{i+j} \tag{2}$$

$$Y_{tCMA_t} = mY_i \tag{3}$$

$$Y_{cCMA_t} = Y_i - mY_i \tag{4}$$

where Y_i is the original crop yield for the *i*th year; and mY_i is the 5-year moving averaged crop yield for the *i*th year; $i = 1,2, \ldots, n$; Y_{tCMAi} and Y_{cCMAi} are the trend yield and climate yield for the *i*th year, respectively.

$$SI = -Y_{cCMA} \tag{5}$$

Table 2
Climate variables for calculating exposure index.

	Indicator Name	Definition	Unit
CDD	Maximum length of dry spell	Maximum number of consecutive days with rainfall <1 mm	Days
CWD	Maximum length of wet spell	Maximum number of consecutive days with rainfall ≥1 mm	Days
rSPEI	Relative standardized precipitation evapotranspiration index of Apr.-Nov.	It characterizes drought by standardizing the difference between precipitation and potential evapotranspiration.	
TX90P	Percentage of days when *TX* (daily maximum temperature) > 90th percentile	Let TX_{ij} be the daily maximum temperature on day *i* in period *j* and let $TX_{in}90$ be the calendar day 90th percentile centred on a 5-day window for the base period 1961–1990. The percentage of time for the base period is determined where: $TX_{ij} > TX_{in}90$	%
FD	Number of frost days	Annual count of days when daily minimum temperature < 0 °C.	Days
Tmean	The change in daily temperature	Average value of daily Tmean	°C

$$AC = Y_{tCMA} \tag{6}$$

To identify whether different detrending approaches affect the results of vulnerability assessment, we also used another two detrending methods, HP Filter (HP) (Eq. S1-S2) and first difference (FD) (Eq. S3-S5), to evaluate the vulnerability of wheat yield in the NSW wheat belt. We only showed the results using the CMA detrending method in the main text. The calculation details of the other two detrending methods were provided in our supplementary material.

Since *EI*, *SI*, and *AC* had different orders of magnitude, we used Eq. (7) to standardize *EI*, *SI*, and *AC*, respectively (Wang and Zhang, 2009). Meanwhile, this equation was applicable to all data standardization in this study.

$$M_i^{'} = \frac{M_i - M_{\min}}{M_{\max} - M_{\min}} \tag{7}$$

where $M_i^{'}$ is the i element of time series $\{M_1, M_2, \ldots, M_n\}$ after standardization; M_i is the i element of time series $\{M_1, M_2, \ldots, M_n\}$ before standardization; $M_{\min} = \min\{M_1, M_2, \ldots, M_n\}$, $M_{\max} = \max\{M_1, M_2, \ldots, M_n\}$.

$$EI = \sum_{i=1}^{n} W_i S_i \tag{8}$$

where W_i is the weighting value of the *i*th indicators (the weighting method of six climate indices was shown in 2.3); and S_i is the value of the *i*th indicators. We first normalized S_i using Eq. (7) (see above) to make it dimensionless and then used derived weight to calculate *EI* (Eq. (8)).

After *EI*, *SI*, and *AC* were obtained, *VI* was calculated according to:

$$VI = SI + EI - AC \tag{9}$$

2.3. Calculation for climate exposure

We first calculated CDD, CWD, rSPEI, TX90P, FD, and Tmean for each climate sites. The 940 sites were assigned into each shire based on the boundary of the shire. The number of climate sites in each shire was shown in Table S2. Then, the CDD, CWD, rSPEI, TX90P, FD, and Tmean for climate sites within each shire were averaged respectively. Here, we followed a previous study of Feng et al. (2018) to predict Y_c based on these six climate indices with random forest (RF) model (Table 2).

RF is a non-parametric technology based on classification and regression trees proposed by Breiman (2001). It uses bootstrap resampling technology to repeatedly extract k samples from the original training sample set N to generate a new training sample set, then generates k classification trees to form a random forest according to the self-service sample set. Finally, the prediction result is obtained by the voting score of the classification tree (Breiman, 2001). In addition, random forest has a great advantage when classifying data: it can give the importance score of each variable in the classification process, according to the score, and it can screen out the relatively important variables. At the same time, the higher importance score of a variable, the more capable it is to classify outcome variables. RF has been widely applied to agricultural and meteorological research due to the high precision, tolerance of abnormal value, and ability to model complex interactions between variables (Feng et al., 2018; Jeong et al., 2016). The default parameters of RF (ntree = 500 and mtry = 3) were used in our analysis. The "%IncMSE" metric was used to calculate relative importance of each index. When the variables were randomly replaced, the %IncMSE represented the average increase of the mean square error of the nodes using a variable in the RF model.

Our RF model had a good performance in predicting Y_c with R^2 of 0.89 and nRMSE of 7%. Then, we used the standardized importance values of CDD, CWD, rSPEI, TX90P, FD, and Tmean derived by RF model (Table S1) as the weight of each index for calculating the exposure of each shire (Eq. (8)).

2.4. Statistical tests

Statistical analysis of *EI*, *SI*, *AC,* and *VI* in time series is helpful to understand their long-term change process under climate change conditions, and to identify their regular characteristics and change trends. We used Mann-Kendall (MK) trend test and continuous wavelet transform (CWT) to identify temporal characteristics of *EI*, *SI*, *AC,* and *VI* in three sub-regions and the whole NSW wheat belt from 1924 to 1998. The M-K test was used to analyze data collected over time for consistently increasing or decreasing trends (monotonic) in *Y* values. CWT can identify the periodic signal of data in time series (Torrence and Compo, 1998; Zeri et al., 2019), and it was used as a supplementary test method for data without significant change trend by numerous researchers (Beecham and Chowdhury, 2010; Li et al., 2019). In addition, *EI*, *SI*, *AC*, and *VI* were derived from climatic factors and wheat yield, which may have obvious inter-annual fluctuation in time series. Therefore, it is necessary to investigate the fluctuation status of these indicators to test whether they have periods with the CWT analysis.

2.4.1. Mann-Kendall trend test

MK test is a non-parametric trend test method (Mann, 1945; Kendall, 1975), which is often used to evaluate the statistical significance of time series trends. Its advantage is its ability to test linear or nonlinear trends. In addition, MK test is less sensitive to the distribution type of data, and also can deal with missing and abnormal values of data. In MK test, the statistic S and the standardized test statistic Z_{MK} were calculated as follows (Sang et al., 2014; Sayemuzzaman and Jha, 2014):

$$S = \sum_{i=1}^{n-1} \sum_{j=i+1}^{n} sgn\left(X_j - X_i\right) \tag{10}$$

$$sgn\left(X_j - X_i\right) = \begin{cases} +1 if \left(X_j - X_i\right). > 0 \\ 0 if \left(X_j - X_i\right) = 0 \\ -1 if \left(X_j - X_i\right). < 0 \end{cases} \tag{11}$$

$$Var(S) = \frac{1}{18}\left[n(n-1)(2n+5) - \sum_{p=1}^{q} t_p\left(t_p - 1\right)\left(2t_p + 5\right)\right] \tag{12}$$

$$Z_{MK} = \begin{cases} \dfrac{S-1}{\sqrt{Var(S)}} if S > 0 \\ 0 if S = 0 \\ \dfrac{S+1}{\sqrt{Var(S)}} if S < 0 \end{cases} \tag{13}$$

where X_i and X_j are the corresponding data values of i and j in the time series ($j > i$); n is the length of the data set; t_p is the number of data in the tied group. A Positive value of Z_{MK} indicates an increasing trend in time series, while a negative Z_{MK} value shows a decreasing trend. When $|Z_{MK}| > Z_{(1-\alpha/2)}$, there is a significant trend in time series. The $Z_{(1-\alpha/2)}$ value can be found in the standard normal distribution table. At the 5% and 1% significance level (95% or 99% confidence intervals), time series trends are significant if $|Z_{MK}| > 1.96$ and $|Z_{MK}| > 2.58$ (Han et al., 2018).

2.4.2. Wavelet analysis

CWT is widely used to identify the statistical characteristics of climate-related indicators in time series. Morlet wavelet is used in this study (Rossi et al., 2011; Roushangar et al., 2018):

$$\psi_0(\eta) = \pi^{-1/4} e^{i\omega_0\eta} e^{-\eta^2/2} \tag{14}$$

where ω_0 is dimensionless frequency with a value of 6 here; η ($\eta = s*t$) is dimensionless time, s is the time scale.

Continuous wavelet transform of time series (x_n, $n = 1, \ldots$, N) with uniform time step (δ_t) can be defined as the convolution of x_n and wavelet normalization (Grinsted et al., 2004). It is defined as:

$$W_n^X(s) = \sqrt{\frac{\delta t}{s}} \sum_{n'=1}^{N} x_{n'} \psi_0\left[(n' - n)\frac{\delta t}{s}\right] \tag{15}$$

where n is the localized time index; n' is the time variable.

2.5. Kernel density plot

Kernel density plot is used to display the distribution of data in x-axis continuous data segments. This plot is a variant of the histogram, using a smooth curve to draw horizontal values. The advantage of kernel density plot over histogram is that it is not affected by the number of grouped data and can better show the distribution shape.

We divided the NSW wheat belt into three sub regions (Fig. 1 and Table 1), and then calculated the average values for *EI*, *SI*, *AC*, and *VI* in the 1930s, 1950s, 1970s, and 1990s in each subregion. The "ggplot2" package in R software was used to make kernel density plot.

2.6. Classification for EI, SI, AC, and VI

We divided these indices into five evaluation grades (Table 3) to clearly describe the changes of *EI*, *SI*, *AC*, and *VI* of 66 shires in NSW wheat belt in different historical periods.

Table 3
The value interval of different *EI*, *SI*, *AC*, and *VI* assessment levels.

Indicators	Very Low	Low	Moderate	High	Very high
Exposure (*EI*)	$EI < 0.10$	$0.10 \le EI < 0.30$	$0.30 \le EI < 0.50$	$0.50 \le EI < 0.70$	$EI \ge 0.70$
Sensitivity (*SI*)	$SI < 0.47$	$0.47 \le SI < 0.57$	$0.57 \le SI < 0.67$	$0.67 \le SI < 0.77$	$SI \ge 0.77$
Adaptive Capacity (*AC*)	$AC < 0.10$	$0.10 \le AC < 0.30$	$0.30 \le AC < 0.50$	$0.50 \le AC < 0.70$	$AC \ge 0.70$
Vulnerability (*VI*)	$VI < 0.20$	$0.20 \le VI < 0.40$	$0.40 \le VI < 0.60$	$0.60 \le VI < 0.80$	$VI \ge 0.80$

3. Results

3.1. Descriptive statistics of wheat yield and climate variables

The long-term wheat yield of the three sub-regions and the whole region showed an obvious increase trend (Fig. 2). Y_c had a great inter-annual fluctuation in all sub regions, and the fluctuation range of region I was the largest from about −2.1 to 1.7 t/ha. From 1924 to 1998, the fluctuation range of Y_c gradually increased indicating that the impact of historical climate on wheat yield was gradually intensified. There were small differences in Y_c obtained by three detrending methods. Note that for FD method, the Y_c fluctuated more than that of another two methods in all sub regions. For the six climate indices, they all had large inter-annual fluctuations (Fig. 3), but there was no significant trend of increasing or decreasing except CWD and rSPEI showing an upward trend.

3.2. Exposure

Spatially, the exposure level of NSW wheat belt gradually decreased from northwest to southeast (Fig. 4 a-d). The number of shires with low and very low exposure increased from 34 to 40 and 1 to 13, respectively. Conversely, the number of shires with moderate, high, and very high exposure decreased gradually from 1930s to 1990s, that is, from 20 to 8, 6 to 4, and from 4 to 1, respectively. According to the kernel density plots of exposure (Fig. 5 a-d), for three sub-regions and the whole region, the density distribution curve and the average value line of exposure showed an overall slight leftward translation trend. The exposure was decreasing from 1930s to 1990s. In addition, the peak value of exposure density was the lowest in region I, which meant that the differences of exposure level among different shires in region I were quite large. The peak in region II, region III, and the whole region were obviously higher than that in region I. For the three sub-regions, from 1924 to 1998, the variation of exposure showed large inter-annual fluctuations (Fig. 6 a-d). The exposure of region I was the highest and had the largest fluctuation during the whole study period. It fluctuated from 0.2–0.8. However, there was a decreasing trend from 1924 to 1998. The temporal changes of exposure in region II and region III were similar, about 0.1–0.6.

3.3. Sensitivity

Fig. 4 e-h showed that the spatial distribution of sensitivity level in different study periods was varied. In 1930s, the sensitivity of wheat belt gradually increased from northwest to southeast. In 1950s, the sensitivity was the lowest as a whole. There were no shires with high and very high sensitivity, and the sensitivity in the western areas was higher than that in the east. In 1970s, the sensitivity of the whole wheat belt was relatively higher. There were 26 shires with high sensitivity. In 1990s, the number of shires with high sensitivity increased sharply from 1 in 1930s to 13 in 1970s, and they were mainly distributed in the southern NSW wheat belt. There were also obvious differences in kernel density plots of the sensitivity in different sub-regions (Fig. 5 e-h). However, for all sub-regions, the sensitivity in 1950s had the highest peak value and the lowest average value. This showed that in 1950s, the sensitivity level was the lowest in all regions, and the sensitivity differences among different shires were also small. For region I, the average sensitivity from 1930s to 1990s was about 0.6, and the sensitivity differences among different shires were small. For region II and region III, the average sensitivity values in 1930s, 1970s, and 1990s were all about 0.6, and the peak of density decreased gradually with time. That is to say, the sensitivity levels of different shires were gradually polarized. In 3 sub-regions, the sensitivity changed similarly with time (Fig. 6 e-h), fluctuating between 0.25 and 0.75. Its inter-annual variation was quite large.

We found that the spatial distribution of sensitivity obtained by different detrending methods was quite different (Fig. 4, Fig. S1, and Fig. S2). For CMA method, the high climate sensitivity of the whole NSW wheat belt appeared in 1970s and 1990s, while that of FD method appeared in 1950s and 1990s, and HP method only generated high sensitivity in 1950s. For each study period, there were also differences in the spatial distribution of sensitivity among the three methods. Take 1950s as an example, the sensitivity based on CMA method was higher in the northwest of the NSW wheat belt, that obtained by HP method was higher in the middle area, and the sensitivity based on FD method was the highest in the southern wheat belt. According to density plots (Fig. 5, Fig. S3, and Fig. S4), the sensitivity value in different detrending methods also had large difference in all regions. The order of peak values of sensitivity density of the three methods from high to low was $SI_{FD} > SI_{CMA} > SI_{HP}$. In addition, the sensitivity value of three methods showed no significant trend from 1924 to 1998 in line plots. They all had great inter-annual fluctuations during the whole study period, and the magnitudes of fluctuation increased with time. However, the magnitudes of the fluctuation (*MF*) of three methods were obviously varied and ordered as $MF_{FD} > MF_{CMA} > MF_{HP}$ (Fig. 6, Fig. S5, and Fig. S6).

3.4. Adaptive capacity

The adaptive capacity increased gradually from 1930s–1990s in NSW wheat belt (Fig. 4 i-l). The number of shires with low and very low adaptive capacity declined from 57 to 2, while the number of shires with high and very high adaptive capacity rose from 0 to 47. The spatial distribution of adaptive capacity for the wheat belt was consistent, which increased gradually from west to east. From 1930s to 1990s, the kernel density curve and mean value line of adaptive capacity for all regions shifted from left to right overall (Fig. 5 i-l), indicating an increasing trend in all regions of the study area. However, the adaptive capacity of region I was lower than that of region II and region III in each year period. Moreover, since the 1950s, the growth rate of adaptive capacity became lower than that of the other two sub-regions. For all regions, the peak value in 1950s was the highest, and the peaks of adaptive capacity in 1930s, 1970s, and 1990s gradually decreased with time. This indicated that the gap in adaptive capacity between different shires decreased rapidly from 1930s to 1950s, and had gradually increased since 1950s. The adaptive capacity of the three sub-regions in NSW wheat belt had an obvious increasing trend in time series (Fig. 6 i-l). The adaptive capacity level of region I increased from 0.1 to 0.5, and that of region II and region III increased more, both from about 0.2 to 0.75. At the same time, the extreme values of the adaptive capacity level of region II and region III were slightly larger than that of region I in the whole time series.

We found that the adaptive capacity obtained by three methods all showed a similar spatial distribution, and gradually increased from northwest to southeast (Fig. 4, Fig. S1, and Fig. S2). According to the kernel density plots, the distribution characteristics of adaptive capacity obtained by the three methods were also similar, and the adaptive capacity increased gradually from 1930s to 1990s (Fig. 5, Fig. S3, and Fig. S4). Meanwhile, the adaptive capacity based on three detrending methods significantly increased from 1924 to 1998 in all regions. However, the magnitude of their inter-annual fluctuation showed differences in three detrending methods, ordered in $MF_{FD} > MF_{CMA} > MF_{HP}$ (Fig. 6, Fig. S5, and Fig. S6).

3.5. Vulnerability

According to the spatial distribution of vulnerability in NSW wheat belt (Fig. 4 m-p), the vulnerability was decreasing from northwest to southeast. Meanwhile, from 1930s to 1990s, the vulnerability of the whole region also decreased. The number of high and very high vulnerable shires reduced from 39 to 4, and these shires were mainly located in the western and northern part of the wheat belt. The number of shires with moderate vulnerability increased by 20 from 1930s to 1950s, but gradually decreased by 29 after 1950s. Moderately vulnerable shires were mainly located in the centre of the study area. The

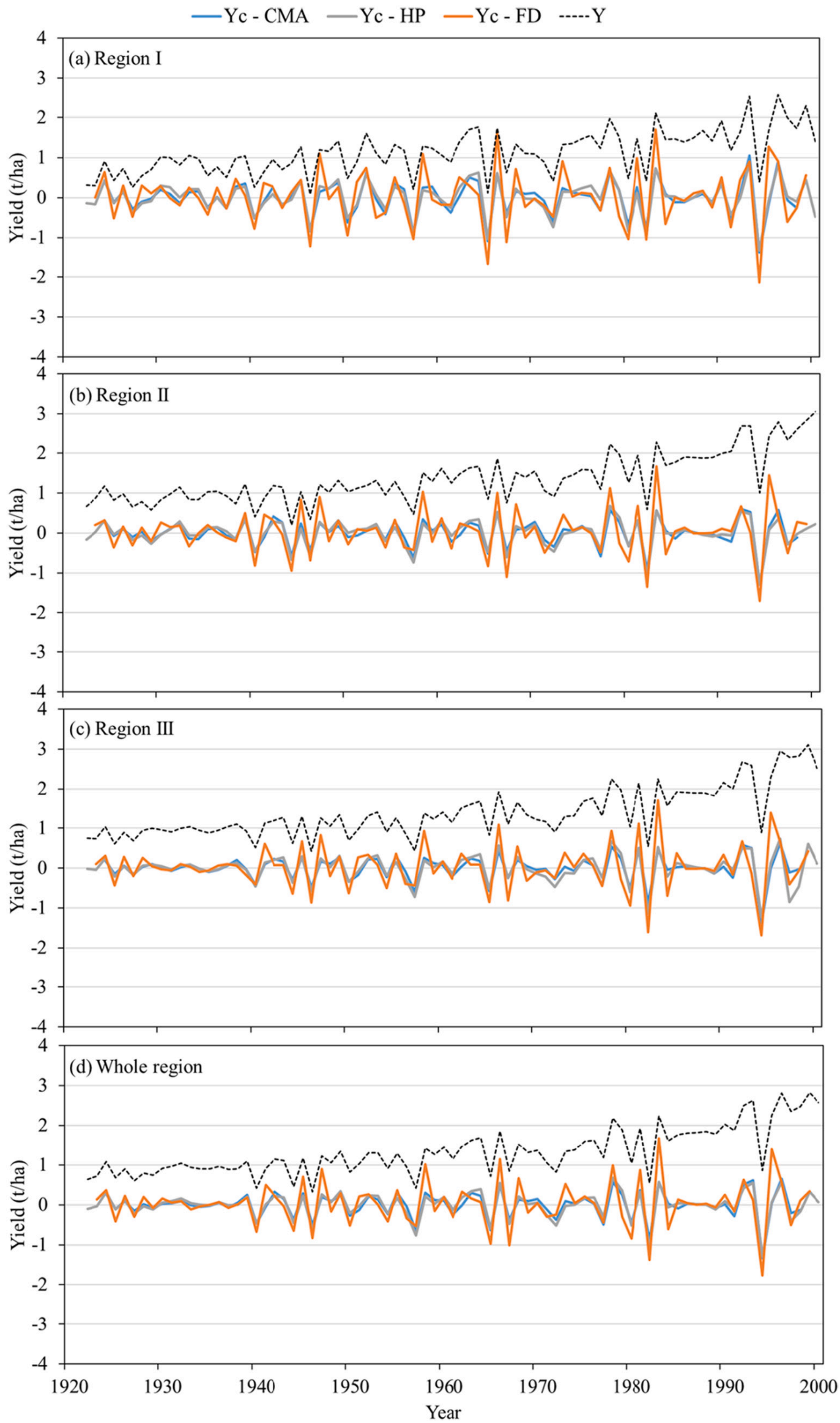

Fig. 2. Averaged observed (Y) and detrending (Y_c) wheat yields obtained by CMA, HP, and FD methods in three sub regions and the whole NSW wheat belt.

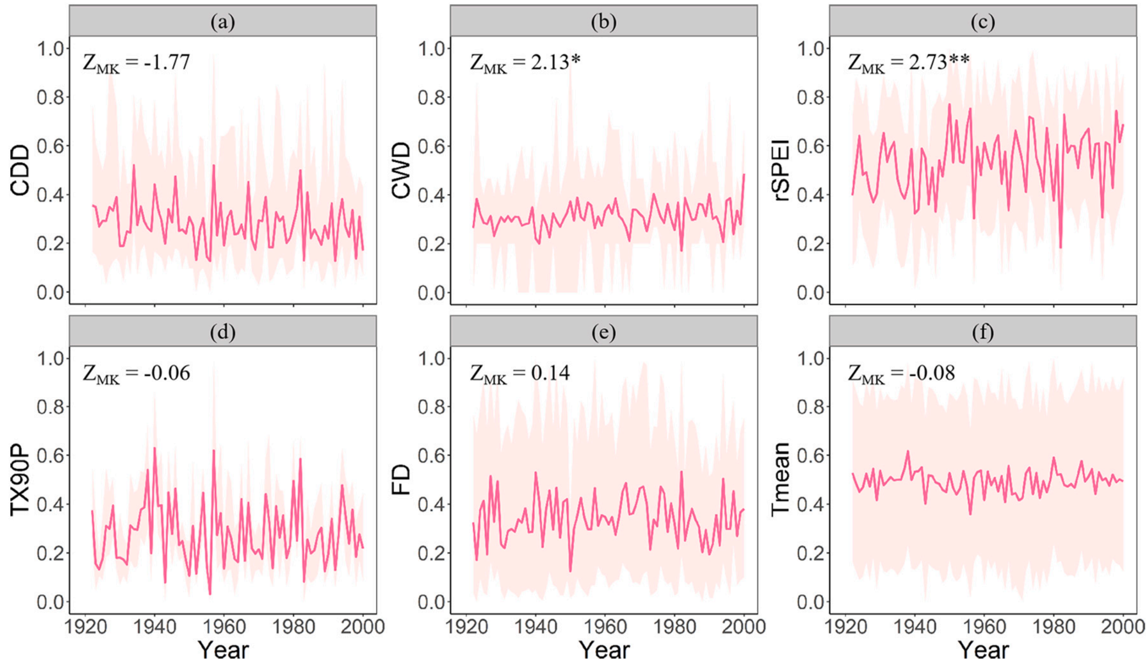

Fig. 3. Averaged value of standardized CDD, CWD, rSPEI, TX90P, FD, and Tmean in 66 shires of the NSW wheat belt.

number of low and very low vulnerable shires increased from 0 in 1930s to 47 in 1990s.

According to the kernel density plots of vulnerability (Fig. 5 m-p), from 1930s to 1990s, the density curve and mean value line in three sub-regions and the whole region showed a trend of overall translation to the left. We conclude that the vulnerability of the NSW wheat belt was decreasing. At the same time, we can know that the density curve and mean line of vulnerability in region I were basically between 0.2 and 1.0 and 0.5–0.8, respectively, and this was obviously higher than those between 0 and 0.8 and 0.2–0.6 in regions II and III, respectively. This revealed that the vulnerability of region I was higher than that of region II and region III during the whole historical period. In addition, the peak value of vulnerability kernel density in different regions had little difference, which increased slightly from 1930s to 1950s, and gradually decreased after 1950s. We infer that, apart from 1950s, the vulnerability difference among different shires in all regions increased gradually from 1930s to 1990s.

For the three sub-regions, vulnerability all decreased from 1924 to 1998, although its inter-annual differences were relatively large (Fig. 6 m-p). The vulnerability of region I was the highest and had the largest fluctuation during the study period. The average vulnerability of region I decreased from 0.9 to 0.4, which was greater than that of region II and region III, decreasing from 0.8 to 0.3. In all sub-regions, the maximum inter-annual variation of vulnerability occurred after 1980. Meanwhile, during 1960 to 1998, the extreme value of the vulnerability level increased obviously, which indicated that the difference of the vulnerability level of different shires increased. However, for region III, the vulnerability difference among different shires was small, only the minimum vulnerability range in the last 20 years has widened. We think that the vulnerability of different shires in region III was similar from 1924 to 1980, while that of low vulnerability shires were lower from 1980 to 1998.

We found that the spatial distributions of vulnerability obtained by the three detrending methods were similar, gradually decreasing from northwest to southeast throughout the NSW wheat belt (Fig. 4, Fig. S1, and Fig. S2). The kernel density of vulnerability based on three methods in different sub regions also showed a similar trend, which gradually decreased from 1930s to 1990s (Fig. 5, Fig. S3, and Fig. S4). In addition, the vulnerability derived from the three detrending methods significantly decreased from 1924 to 1998, and showed inter-annual fluctuation in different amplitudes (Fig. 6, Fig. S5, and Fig. S6).

We used MK test to analyze the trends of exposure, sensitivity, adaptive capacity, and vulnerability (Fig. 6 a-p). Meanwhile, the time and period characteristics of these four indicators were combined by continuous wavelet transform (Fig. 7). The exposure showed a slight decreasing trend in three sub-regions and the whole region, but only the exposure of region I had passed the significance test (Fig. 6 a-d). At the same time, the results of wavelet analysis showed that the high frequency part (HFP) of exposure was mainly distributed in 0-10a in three sub-regions, and the wavelet power spectrum energy changed discontinuously in HFP. Among them, region I and region III had an 8-10a period passed the significance test in 1930s, while the period of significance for region II was 4-6a in 1972 (Fig. 7 a-d). Sensitivity level had no significant change trend in all regions (Fig. 6 e-h). However, its periodicity was obvious, and had a main oscillation period of 4.5–7.7a in all regions. The HFP mainly concentrated in 0–7.7a, but the change was discontinuous. In addition, in region I and region III, there were 2-6a periods in 1941–1960 and 1996, had passed the significance test. The periods of significance for region III were shorter, mainly concentrated in 1978 and 1996 (Fig. 7 e-h). Adaptive capacity in different regions all had significantly increased (Fig. 6 i-l), while the periodicity was not significant, and the HFP existed only in 11.2–16.5a of region I (Fig. 7 i-l). The vulnerability of the three sub-regions and the whole region decreased significantly with time (Fig. 6 m-p). The results of wavelet analysis showed that the HFP of vulnerability in different regions was mainly between 0 and 3.6a. In 1966, 1978 and 1996, there were short periods of 0–1.8a, which passed the significance test. Also, region I had a significant short period of 2–3.6a in 1954 (Fig. 7 m-p).

To sum up, the trend and periodicity of data can supplement each other. Taking adaptive capacity as an example, it had an obvious increasing trend with a weak periodic signal in the time series across the three subregions and the whole NSW wheat belt. Meanwhile, the data with large inter-annual fluctuations, such as exposure, had discontinuous periods in the time series.

4. Discussion

Our study used a comprehensive index method to assess the

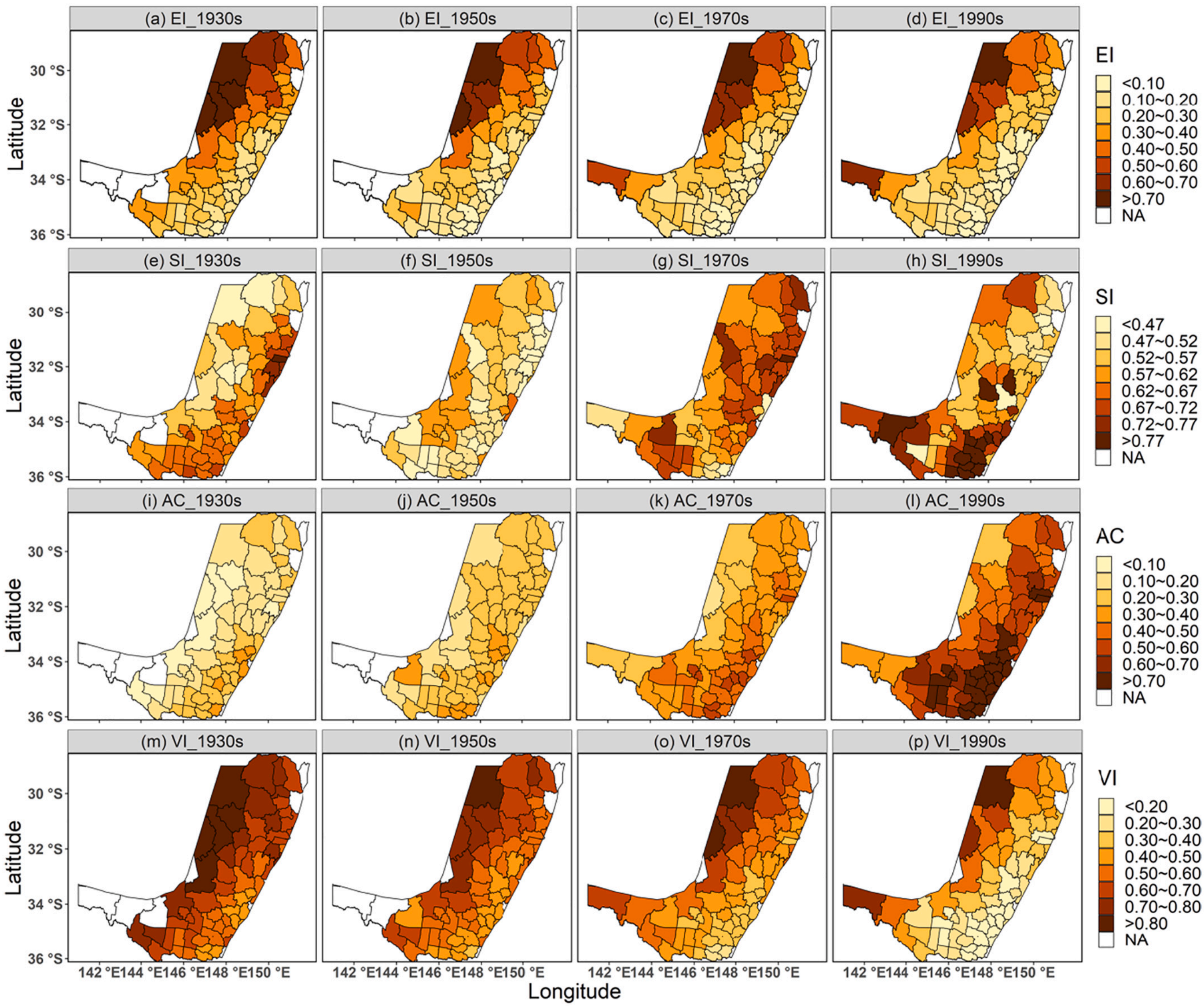

Fig. 4. Spatial distribution of *EI*, *SI*, *AC*, and *VI* in NSW wheat belt for 1930s, 1950s, 1970s, and 1990s based on CMA method.

vulnerability of wheat yield to climate change. We used the trend of historical yield as proxy of adaptive capacity, which considered the contribution of management, socio-economic, and technological progress to crop yield (Franke et al., 2019; Bogunovic et al., 2018; Adimassu and Kessler, 2016; Olesen et al., 2011). Sensitivity was represented by detrending yield, which characterized the final result of wheat affected by climate variability and extreme weather events. Furthermore, we developed a RF model to predict detrending yield based on six representative climate indices. The variable importance derived from RF was used to give the weight of six climate indices. Then the weighted sum of the six climate indices represented exposure. The exposure index we developed here considered the average changes and extreme events of rainfall and temperature.

Sensitivity and exposure are both related to climate factors. The differences between them are: when assessing the vulnerability of agricultural system to climate change, exposure is essentially the magnitude of extrinsic change in climate itself. Conversely, sensitivity is the amount of corresponding change to these given amount of exposure (Kling et al., 2020). Note that the regions with high sensitivity are not always the ones with high exposure. For example, in 1930s, 1950s, and 1990s, the value of sensitivity for those shires in the eastern and southern parts of wheat belt was higher than that in northwestern areas, where exposure was the highest during the whole study period (Fig. 4).

Most previous studies regarding the impact of historical climate on crops often use different detrending methods to remove non-climatic yield (Y_t). Then only climatic yield (Y_c) and different climate variables were used to establish the relationship between crops and climate change. They identified dominant climatic drivers that determine yield variations (e.g., Wang et al., 2015). In this study, we not only separated Y_c and Y_t, but also used both Y_c and Y_t to conduct vulnerability analysis. Our vulnerability index can not only reflect the impact of climate on crop production system, but also consider the resilience of the system itself. This comprehensive assessment is very helpful for locating those areas that are unable to cope with adverse climate impacts, which often have high sensitivity and exposure, and low adaptive capacity. This method is more helpful to the planning of adaptation measures and the rational allocation of agricultural resources, compared with studies only considering the effects of climate factors.

We demonstrated that the vulnerability gradually decreased from 1924 to 1998. Exposure and sensitivity did not increase or decrease significantly throughout the study periods, although they fluctuated greatly from year to year. However, the adaptive capacity significantly increased with time. We found that the adaptive capacity was increased mainly because of the improvement of agronomic management

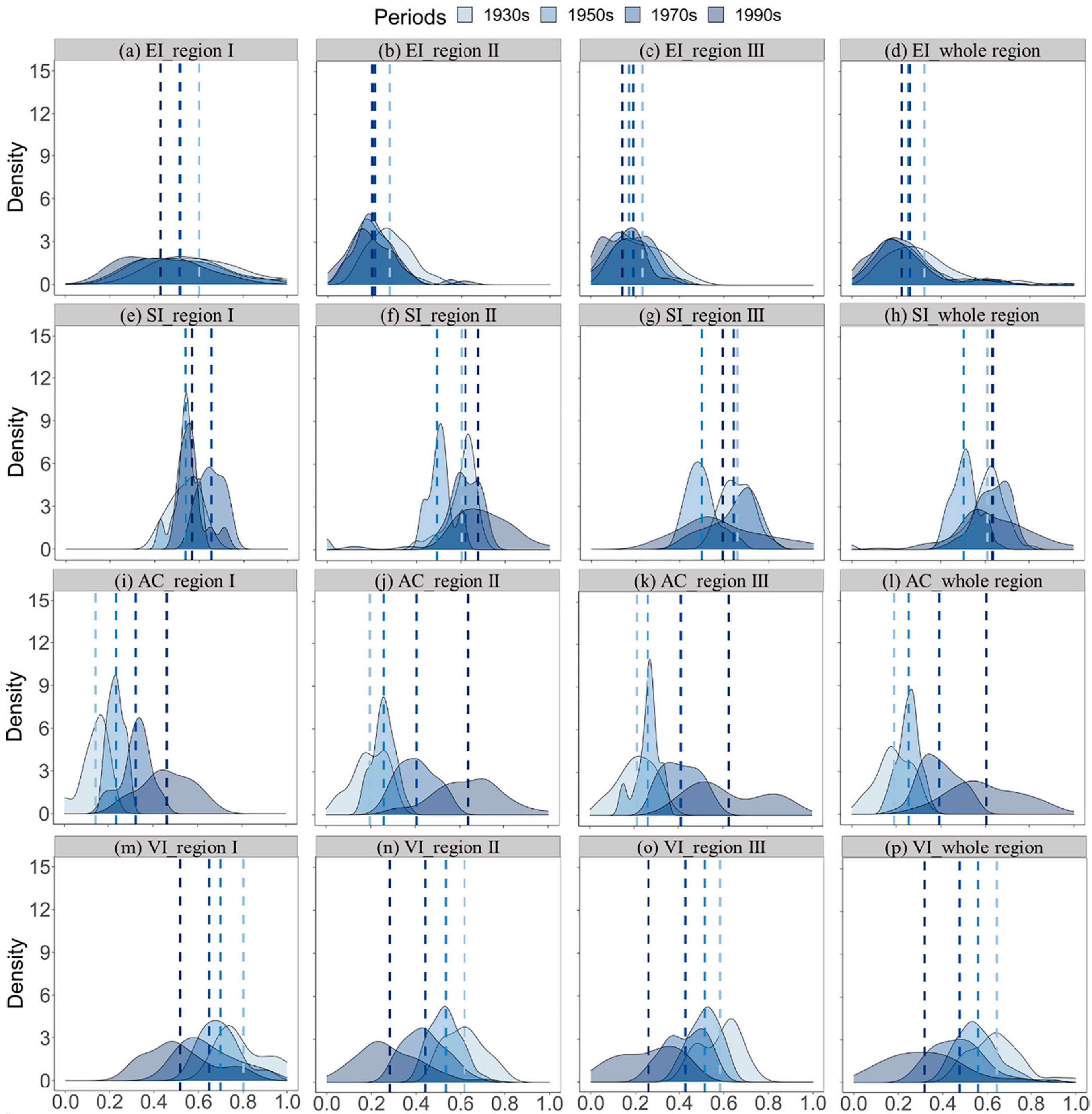

Fig. 5. Kernel density of *EI*, *SI*, *AC*, and *VI* based on CMA method in three sub-regions and the whole NSW wheat belt. The vertical blue dotted line from shallow to deep represent the average value of the indicator in 1930s, 1950s, 1970s, and 1990s, respectively. (For interpretation of the references to colour in this figure legend, the reader is referred to the web version of this article.)

practices, technological, and socio-economic progress. For example, adjusting the sowing date of crops can make crops grow in a more favourable climate condition, avoid frequent risk periods such as heat, frost, and drought, then reduce the adverse effects of climate and weather on crop production (Gomez-Macpherson and Richards, 1995). Furthermore, the emergence of new crop varieties, the application of herbicides and chemical fertilizers improve the productivity of crops (Anderson et al., 2005). In addition, the improvement of agricultural machinery as well as the progress of communication and computer technology have improved the efficiency of agricultural production and the speed and range of farmers receiving information (Kingwell and Pannell, 2005). Finally, the increase of farmers' livelihood capital is also the reason for enhancing adaptive capacity (Huai, 2016). As for sensitivity and exposure, they are highly correlated with climate conditions. The climate indices had large inter-annual fluctuations (Fig. 3) with no significant trend of increasing or decreasing except CWD and rSPEI.

Spatially, we found that the vulnerability of region I, located in the northwest of the wheat belt, was about 0.45–0.80, higher than the 0.24–0.60 of the other two sub-regions. At the same time, from 1930s to 1990s, the vulnerability of region II was slightly higher than that of region III, but the difference was small. The main reason was that, under the condition of small difference in sensitivity among the three sub-

Fig. 6. The annual averaged value of *EI*, *SI*, *AC*, and *VI* based on CMA method in three sub-regions and the whole NSW wheat belt in 1924–1998. The top and bottom boundaries of shaded areas represent the maximum and minimum value, respectively. Z_{MK} is the increasing (decreasing) rate of *EI*, *SI*, *AC*, and *VI* during the period from 1924 to 1998 in three sub-regions and the whole NSW wheat belt (*** $p < 0.001$, ** $p < 0.01$, * $p < 0.05$).

regions, the exposure of region I was the highest (Fig. 5), while its adaptive capacity was the lowest (Fig. 5). Climate conditions in region I were less favourable for wheat growth than other two regions (Fig. 5 a). For example, compared with the southeast, the northwest of wheat belt has less precipitation and higher temperature (Feng et al., 2019b). This dry and hot climate tends to aggravate the adverse effects on wheat production (Wang et al., 2020). Moreover, the rainfall pattern in the northwest is mainly summer dominant, which means that the main rainfall does not fall in the wheat growth period, resulting in less available water for wheat in the northwest. On the contrary, rainfall in southwest is generally uniform or winter dominant (Wang et al., 2018), therefore, wheat in this area can use more effective precipitation. In region I, we mainly attributed the lowest adaptive capacity to the poorest accessible to natural, financial, and physical resources in the northwestern NSW compared with other regions (Schirmer and Hanigan, 2015).

We highlight the need to assess vulnerability on the shire scale. From shire scale, we found that Warren (ID: 7), Coonamble (ID: 6), Bogan (ID: 8), and Walgett (ID: 1) were the most vulnerable areas based on CMA detrending method, and they were all located in region I. Also, the exposure level of these shires was the highest among 66 shires, while their adaptive capacity was almost the lowest. We suspect that this combination of factors may explain why they had the highest vulnerability. Policy makers and farmers should give priority to the application of effective agricultural adaptation and capital investment in these shires. Farmers can try to plant drought-resistant and heat-resistant wheat, adjust the sowing date of wheat, or use residue mulching to alleviate or eliminate the adverse effects of climate (drought, high temperature, frost, etc.) in these shires. These techniques may improve the adaptive capacity under high exposure (Zhao et al., 2015). Based on the APSIM simulations of the impacts of climate change on wheat production for Walgett, Crimp et al. (2019) suggested choosing new varieties with heat and drought resistance, and altering planting decisions to adapt climate changes. Furthermore, policy makers and farmers should consider whether these shires need to transform and stop growing wheat. This proposal was consistent with the change of farming methods in the crop belt of northern NSW after the 1990s. Taking Walgett as an example, from 1995 to 2001, the planting area of wheat decreased from 85% to 70%, while that of chickpea increased from 2% to 23% (GRDC, 2004).

Conversely, Holbrook (ID: 65), Hume (ID: 66), Harden (ID: 63), and Boorowa (ID: 61) were shires with the lowest vulnerability in the wheat belt based on CMA detrending method. They were all in region III and located in the southeast of the study area. In these shires, the planting

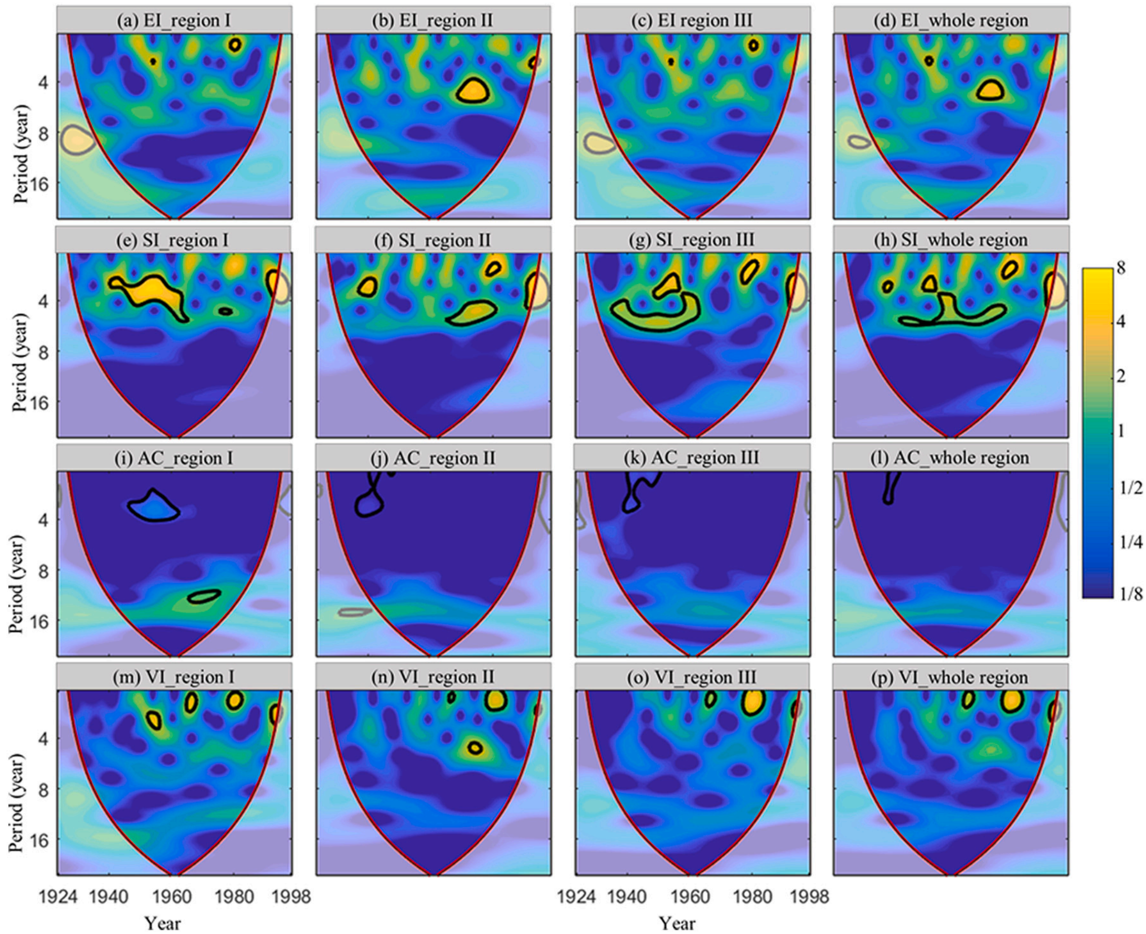

Fig. 7. The wavelet-spectra of annual *EI*, *SI*, *AC*, and *VI* based on CMA method in three sub-regions and the whole NSW wheat belt in 1924–1998. The red line denotes the cones of influence, and the thick solid line shows the 95% confidence level. Yellow and blue area in the figure represent the peak and valley of wavelet energy density, respectively. (For interpretation of the references to colour in this figure legend, the reader is referred to the web version of this article.)

area of wheat should be appropriately increased, so as to make full use of the advantages of low vulnerability, thus increasing the wheat production. Moreover, the agricultural managements practised in these shires can be passed on to other areas with high vulnerability, helping them to reduce the vulnerability of wheat production, so as to achieve stable and sustained growth of wheat yield.

We found that there was no difference among the three detrending methods in locating shires with the highest vulnerability in the NSW wheat belt. The four most vulnerable shires in NSW wheat belt were consistent in the three methods. However, when locating shires with lowest vulnerability, the results obtained by the three detrending methods were different (Holbrook (ID: 65), Hume (ID: 66), Blayney (ID: 60), and Cootamundra (ID: 36) for HP method; Holbrook (ID: 65), Hume (ID: 66), Blayney (ID: 60), and Culcairn (ID: 61) for FD method).

More work are still needed to explore the issues raised in our research. Although we investigated the spatiotemporal changes of exposure, sensitivity, adaptive capacity, and vulnerability in the NSW wheat belt, we did not assess the vulnerability from 2001 to 2021 due to lack of yield data for each shire after 2000. In addition, by comparing the vulnerability results of three detrending methods, we found that different detrending methods can lead to different results in vulnerability assessment spatially. This has been reported by a previous study of Lu et al. (2017), showing detrending methods significantly affect Y_c and Y_t. In addition, Ye et al. (2015) used multiple detrending methods to assess crop yield risk and found that the estimated yield loss rate varied with different detrending methods. Thus, pre-selecting suitable detrending methods according to specific research objectives and contents is necessary to reduce the possibility of significant differences. Understanding the vulnerability of crop yield to historical climate is an indispensable step for assessing the vulnerability of crop productivity to future climate change (Uddin et al., 2019; Wang et al., 2020; Ahmadalipour and Moradkhani, 2018). The drought intensity of NSW wheat belt was predicted to increase in the next few decades, and the drought affected area will expand from west to east (Feng et al., 2019a). Meanwhile, warm days (TX90P) also show an increasing trend, especially in the northeast of wheat belt (Wang et al., 2016). Hence, the exposure in NSW is likely to increase in the future, and the area with high exposure will gradually expand from northwest towards eastern and southern districts. In this case, how will the vulnerability of the east and south of wheat belt change in the future? Can future adaptive capacity offset this increasing exposure? Also, do these regions need to increase additional agricultural adaptation practices and investment, so as to enhance their adaptive capacity? These questions can be answered by assessing vulnerability under future climate change. We expect that our vulnerability assessment method can be combined with process-based crop model driven by global climate models to predict the vulnerability of wheat yield in the future. Therefore, we can determine whether those less vulnerable areas (the eastern and southern parts of the wheat belt) in historical periods can still keep low vulnerability under the future climate change.

5. Conclusion

We used the data of crop yield and climatic indices in 1924–1998, combining with the methods of yield de-trending and comprehensive exposure index to assess wheat yield vulnerability to climate as a case study in south-eastern Australia. We found that, from the 1930s to the 1990s, both exposure and sensitivity had large inter-annual variations without significant increasing or decreasing trend. However, adaptive capacity increased by 34% from 1930s to 1950s, 54% from 1950s to 1970s, and 54% from 1970s to 1990s. The vulnerability in the wheat belt decreased by 13% from 1930s to 1950s, 15% from 1950s to 1970s, and 33% from 1970s to 1990s. This is mainly due to increased adaptive capacity with the improvement of agronomic management practices, technological and socio-economic progress. Our results highlight that the hotspots of wheat yield vulnerability were located in the north-western parts of NSW wheat belt. Our study provides useful information for policymakers to plan and implement the priority adaptations and investments to mitigate the vulnerability in these areas. Meanwhile, policymakers should also find ways to make full use of the favourable conditions in the southeastern NSW wheat belt, so as to improve the state wide potential of wheat productivity.

Our study emphasizes that vulnerability assessment based on crop yield and climate change indices is a useful approach. Additionally by using this method, researchers can assess the vulnerability of crop yield to future climate change in combination with process-based model simulated results. So, we can know whether the exposure and sensitivity will increase significantly under future climate change, and whether the improvement of adaptive capacity can offset their increase. The vulnerability prediction will provide effective guidance for agricultural resource allocation and investment planning, so as to achieve the maximum benefit of agricultural productivity. We highlight the need to apply a simple and universal method for vulnerability assessment. It facilitates the comparison of vulnerability in different regions and the prediction of future vulnerability. This is of great significance to policymakers' precise agricultural management and planning. This information will help industry leaders facilitate change in production systems of several industries, including wheat, to better prepare farmers for climate change and hence, to maintain productivity and profitability into the future.

Declaration of Competing Interest

The authors declare that they have no known competing financial interests or personal relationships that could have appeared to influence the work reported in this paper.

Acknowledgements

The first author acknowledges the China Scholarship Council (CSC) for the financial support for her Ph.D. study. Facilities for conducting this study were provided by the New South Wales Department of Primary Industries. Dr. Bernie Dominiak provided comments on an earlier version of this manuscript.

Appendix A. Supplementary data

Supplementary data to this article can be found online at https://doi.org/10.1016/j.agsy.2021.103340.

References

ABARES, 2021. https://www.agriculture.gov.au/abares/research-topics/agricultural-outlook/data#australian-crop-report-data. The last accessed date: 25 May 2021.
Abson, D.J., Dougill, A.J., Stringer, L.C., 2012. Using principal component analysis for information-rich socio-ecological vulnerability mapping in southern Africa. Appl. Geogr. 35, 515–524.
Adger, W.N., 2006. Vulnerability. Glob. Environ. Chang. 16, 268–281.
Adimassu, Z., Kessler, A., 2016. Factors affecting farmers' coping and adaptation strategies to perceived trends of declining rainfall and crop productivity in the central rift valley of Ethiopia. Environ. Syst. Res. 5, 13.
AEGIC, 2021. https://www.aegic.org.au/australian-grain-production-a-snapshot/. The last accessed date: 20 May 2021.
Ahmadalipour, A., Moradkhani, H., 2018. Multi-dimensional assessment of drought vulnerability in Africa: 1960-2100. Sci. Total Environ. 644, 520–535.
Anderson, W.K., Hamza, M.A., Sharma, D.L., D'Antuono, M.F., Hoyle, F.C., Hill, N., Shackley, B.J., Amjad, M., Zaicou-Kunesch, C., 2005. The role of management in yield improvement of the wheat cropa review with special emphasis on Western Australia. Aust. J. Agric. Res. 56, 1137–1149.
Bandyopadhyay, N., Bhuiyan, C., Saha, A., 2016. Heat waves, temperature extremes and their impacts on monsoon rainfall and meteorological drought in Gujarat, India. Nat. Hazards 82, 367–388.
Beecham, S., Chowdhury, R.K., 2010. Temporal characteristics and variability of point rainfall: a statistical and wavelet analysis. Int. J. Climatol. 30, 458–473.
Bogunovic, I., Pereira, P., Kisic, I., Sajko, K., Sraka, M., 2018. Tillage management impacts on soil compaction, erosion and crop yield in Stagnosols (Croatia). Catena 160, 376–384.
Breiman, L., 2001. Random forests. Mach. Learn. 45, 5–32.
Bryan, B.A., Huai, J., Connor, J., Gao, L., King, D., Kandulu, J., Zhao, G., 2015. What actually confers adaptive capacity? Insights from agro-climatic vulnerability of Australian wheat. PLoS One 10.
Crimp, S., Mahani, M., Howden, M., 2019. Predicted Climate Change Impacts on Northern NSW Farming Systems. https://grdc.com.au/resources-and-publications/grdc-update-papers/tab-content/grdc-update-papers/2019/08/predicted-climate-change-impacts-on-northern-nsw-farming-systems. The last accessed date: 5 May 2021.
Dong, Z., Pan, Z., An, P., Wang, L., Zhang, J., He, D., Han, H., Pan, X., 2015. A novel method for quantitatively evaluating agricultural vulnerability to climate change. Ecol. Indic. 48, 49–54.
Dong, Z., Pan, Z., He, Q., Wang, J., Huang, L., Pan, Y., Han, G., Xue, X., Chen, Y., 2018. Vulnerability assessment of spring wheat production to climate change in the Inner Mongolia region of China. Ecol. Indic. 85, 67–78.
Ericksen, P., Thornton, P., Notenbaert, A., Cramer, L., Jones, P., Herrero, M., 2011. Mapping hotspots of climate change and food insecurity in the global tropics. In: CCAFS Report 5. CCAFS, Copenhagen, Denmark.
Feng, P., Wang, B., Liu, D.L., Xing, H., Ji, F., Macadam, I., Ruan, H., Yu, Q., 2018. Impacts of rainfall extremes on wheat yield in semi-arid cropping systems in eastern Australia. Clim. Chang. 147, 555–569.
Feng, P., Liu, D.L., Wang, B., Waters, C., Zhang, M., Yu, Q., 2019a. Projected changes in drought across the wheat belt of southeastern Australia using a downscaled climate ensemble. Int. J. Climatol. 39, 1041–1053.
Feng, P., Wang, B., Liu, D.L., Waters, C., Yu, Q., 2019b. Incorporating machine learning with biophysical model can improve the evaluation of climate extremes impacts on wheat yield in South-Eastern Australia. Agric. For. Meteorol. 275, 100–113.
Fitzsimmons, R., 2001. Winter Cereal Production Statistics, NSW 1922–1999: Wheat, Oats, Barley: Area Production and Yield: NSW by Local Government Areas, Individual Years plus 5 and 10 Year Averages, 6th edn. Australian Institute of Agricultural Science and Technology, Wahroonga.
Franke, A., Baijukya, F., Kantengwa, S., Reckling, M., Vanlauwe, B., Giller, K.E., 2019. Poor farmers–poor yields: socio-economic, soil fertility and crop management indicators affecting climbing bean productivity in northern Rwanda. Exp. Agric. 55, 14–34.
Gbetibouo, G.A., Ringler, C., Hassan, R., 2010. Vulnerability of the south African farming sector to climate change and variability: an indicator approach. Nat. Res. Forum 34, 175–187.
Gomez-Macpherson, H., Richards, R., 1995. Effect of sowing time on yield and agronomic characteristics of wheat in South-Eastern Australia. Aust. J. Agric. Res. 46, 1381–1399.
GRDC, 2004. DAN459 - Western Farming Systems Project - NSW Agriculture Component. 2000-2004. https://grdc.com.au/research/reports/report?id=198. The last accessed date: 5 May 2021.
Grinsted, A., Moore, J.C., Jevrejeva, S., 2004. Application of the cross wavelet transform and wavelet coherence to geophysical time series. Nonlinear Process. Geophys. 11, 561–566.
Han, J., Wang, J., Zhao, Y., Wang, Q., Zhang, B., Li, H., Zhai, J., 2018. Spatio-temporal variation of potential evapotranspiration and climatic drivers in the Jing-Jin-Ji region, North China. Agric. For. Meteorol. 256-257, 75–83.
Hinkel, J., 2011. "Indicators of vulnerability and adaptive capacity": towards a clarification of the science–policy interface. Glob. Environ. Chang. 21, 198–208.
Hochman, Z., Gobbett, D.L., Horan, H., 2017. Climate trends account for stalled wheat yields in Australia since 1990. Glob. Chang. Biol. 23, 2071–2081.
Howden, S.M., Soussana, J.F., Tubiello, F.N., Chhetri, N., Dunlop, M., Meinke, H., 2007. Adapting agriculture to climate change. Proc. Natl. Acad. Sci. U. S. A. 104, 19691–19696.
Huai, J., 2016. Role of livelihood capital in reducing climatic vulnerability: insights of Australian wheat from 1990–2010. PLoS One 11, e0152277.
IPCC, 2007. Climate Change 2007: Impacts, Adaptation, and Vulnerability. Contribution of Working Group II to the Fourth Assessment Report of the Intergovernmental Panel on Climate Change. Cambridge University Press, Cambridge, U.K.
IPCC, 2012. Managing the Risks of Extreme Events and Disasters to Advance Climate Change Adaptation. Special Report of the Intergovernmental Panel on Climate Change. Journal of Clinical Cambridge University Press, Cambridge, U.K.
Jeffrey, S.J., Carter, J.O., Moodie, K.B., Beswick, A.R., 2001. Using spatial interpolation to construct a comprehensive archive of Australian climate data. Environ. Model. Softw. 16, 309–330.

Jeong, J.H., Resop, J.P., Mueller, N.D., Fleisher, D.H., Yun, K., Butler, E.E., Timlin, D.J., Shim, K.-M., Gerber, J.S., Reddy, V.R., Kim, S.-H., 2016. Random forests for global and regional crop yield predictions. PLoS One 11, e0156571.
Kamali, B., Abbaspour, K.C., Lehmann, A., Wehrli, B., Yang, H., 2018a. Spatial assessment of maize physical drought vulnerability in sub-Saharan Africa: linking drought exposure with crop failure. Environ. Res. Lett. 13.
Kamali, B., Abbaspour, K.C., Wehrli, B., Yang, H., 2018b. Drought vulnerability assessment of maize in sub-Saharan Africa: insights from physical and social perspectives. Glob. Planet. Chang. 162, 266–274.
Kendall, M.G., 1975. Rank Correlation Methods. Griffin, London.
Kingwell, R., Pannell, D., 2005. Economic trends and drivers affecting the wheatbelt of Western Australia to 2030. Crop Pasture Sci. 56, 553–561.
Kurukulasuriya, P., Mendelsohn, R., 2008. How Will Climate Change Shift Agro-Ecological Zones and Impact African Agriculture? The World Bank.
Lal, M., Singh, K., Rathore, L., Srinivasan, G., Saseendran, S., 1998. Vulnerability of rice and wheat yields in NW India to future changes in climate. Agric. For. Meteorol. 89, 101–114.
Li, Y., Xiong, W., Hu, W., Berry, P., Ju, H., Lin, E., Wang, W., Li, K., Pan, J., 2014. Integrated assessment of China's agricultural vulnerability to climate change: a multi-indicator approach. Clim. Chang. 128, 355–366.
Li, Y., Huang, H., Ju, H., Lin, E., Xiong, W., Han, X., Wang, H., Peng, Z., Wang, Y., Xu, J., Cao, Y., Hu, W., 2015. Assessing vulnerability and adaptive capacity to potential drought for winter-wheat under the RCP 8.5 scenario in the Huang-Huai-Hai plain. Agric. Ecosyst. Environ. 209, 125–131.
Li, L., Yao, N., Li, Y., Liu, D.L., Wang, B., Ayantobo, O.O., 2019. Future projections of extreme temperature events in different sub-regions of China. Atmos. Res. 217, 150–164.
Lobell, D.B., Schlenker, W., Costa-Roberts, J., 2011. Climate trends and global crop production since 1980. Science 333, 616.
Lu, J., Carbone, G.J., Gao, P., 2017. Detrending crop yield data for spatial visualization of drought impacts in the United States, 1895–2014. Agric. For. Meteorol. 237-238, 196–208.
Mann, H.B., 1945. Nonparametric tests against trend. Econometrica 13, 245–259.
McCarthy, J.J., Canziani, O.F., Leary, N.A., Dokken, D.J., White, K.S., 2001. Climate change 2001: impacts, adaptation, and vulnerability. Contribution of working group II to the third assessment report of the intergovernmental panel on climate change (IPCC). Glob. Ecol. Biogeogr. 12, 87–88.
Neset, T.-S., Wiréhn, L., Opach, T., Glaas, E., Linnér, B.-O., 2019. Evaluation of indicators for agricultural vulnerability to climate change: the case of Swedish agriculture. Ecol. Indic. 105, 571–580.
Olesen, J.E., Trnka, M., Kersebaum, K.C., Skjelvåg, A.O., Seguin, B., Peltonen-Sainio, P., Rossi, F., Kozyra, J., Micale, F., 2011. Impacts and adaptation of European crop production systems to climate change. Eur. J. Agron. 34, 96–112.
Pandey, R., Jha, S.K., Alatalo, J.M., Archie, K.M., Gupta, A.K., 2017. Sustainable livelihood framework-based indicators for assessing climate change vulnerability and adaptation for Himalayan communities. Ecol. Indic. 79, 338–346.
Ray, D.K., Mueller, N.D., West, P.C., Foley, J.A., Hart, J.P., 2013. Yield trends are insufficient to double global crop production by 2050. PLoS One 8, e66428.
Ray, D.K., Gerber, J.S., MacDonald, G.K., West, P.C., 2015. Climate variation explains a third of global crop yield variability. Nat. Commun. 6, 1–9.
Rossi, A., Massei, N., Laignel, B., 2011. A synthesis of the time-scale variability of commonly used climate indices using continuous wavelet transform. Glob. Planet. Chang. 78, 1–13.
Roushangar, K., Alizadeh, F., Adamowski, J., 2018. Exploring the effects of climatic variables on monthly precipitation variation using a continuous wavelet-based multiscale entropy approach. Environ. Res. 165, 176–192.
Sang, Y.F., Wang, Z., Liu, C., 2014. Comparison of the MK test and EMD method for trend identification in hydrological time series. J. Hydrol. 510, 293–298.
Sayemuzzaman, M., Jha, M.K., 2014. Seasonal and annual precipitation time series trend analysis in North Carolina, United States. Atmos. Res. 137, 183–194.
Schirmer, J., Hanigan, I., 2015. Understanding the Resilience of NSW Farmers.
Semenov, M.A., Shewry, P.R., 2011. Modelling predicts that heat stress, not drought, will increase vulnerability of wheat in Europe. Sci. Rep. 1, 66.
Senapati, N., Halford, N.G., Semenov, M.A., 2021. Vulnerability of European wheat to extreme heat and drought around flowering under future climate. Environ. Res. Lett. 16, 024052.
Sendhil, R., Jha, A., Kumar, A., Singh, S., 2018. Extent of vulnerability in wheat producing agro-ecologies of India: tracking from indicators of cross-section and multi-dimension data. Ecol. Indic. 89, 771–780.
Sonkar, G., Mall, R., Banerjee, T., Singh, N., Kumar, T.L., Chand, R., 2019. Vulnerability of Indian wheat against rising temperature and aerosols. Environ. Pollut. 254, 112946.
Sun, C.X., Huang, G.H., Fan, Y., Zhou, X., Lu, C., Wang, X.Q., 2019. Drought occurring with hot extremes: changes under future climate change on loess plateau, China. Earth's Future 7, 587–604.
Torrence, C., Compo, G.P., 1998. A practical guide to wavelet analysis. Bull. Am. Meteorol. Soc. 79, 61–78.
Uddin, M.N., Saiful Islam, A.K.M., Bala, S.K., Islam, G.M.T., Adhikary, S., Saha, D., Haque, S., Fahad, M.G.R., Akter, R., 2019. Mapping of climate vulnerability of the coastal region of Bangladesh using principal component analysis. Appl. Geogr. 102, 47–57.
Wang, H., Zhang, J., 2009. Analysis of different data standardization forms for fuzzy clustering evaluation Results' influence. In: 2009 3rd International Conference on Bioinformatics and Biomedical Engineering, pp. 1–4.
Wang, B., Chen, C., Liu, D.L., Asseng, S., Yu, Q., Yang, X., 2015. Effects of climate trends and variability on wheat yield variability in eastern Australia. Clim. Res. 64, 173–186.
Wang, B., Liu, D.L., Macadam, I., Alexander, L.V., Abramowitz, G., Yu, Q., 2016. Multi-model ensemble projections of future extreme temperature change using a statistical downscaling method in south eastern Australia. Clim. Chang. 138, 85–98.
Wang, B., Liu, D.L., Asseng, S., Macadam, I., Yang, X., Yu, Q., 2017. Spatiotemporal changes in wheat phenology, yield and water use efficiency under the CMIP5 multimodel ensemble projections in eastern Australia. Clim. Res. 72, 83–99.
Wang, B., Liu, D.L., Waters, C., Yu, Q., 2018. Quantifying sources of uncertainty in projected wheat yield changes under climate change in eastern Australia. Clim. Chang. 151, 259–273.
Wang, B., Feng, P., Liu, D.L., Waters, C., 2020. Modelling biophysical vulnerability of wheat to future climate change: a case study in the eastern Australian wheat belt. Ecol. Indic. 114, 106290.
Watson, R.T., Zinyowera, M.C., Moss, R.H., 1996. Climate Change 1995:Impacts, Adaptations and Mitigation of ClimateChange:Scientific—Technical Analyses. Cambridge University Press.
Watson, R.T., Zinyowera, M.C., Moss, R.H., Dokken, D.J., 1997. IPCC Special Report on the Regional Impacts of Climate Change – An Assessment of Vulnerability. Cambridge University Press, Cambridge.
Yang, X., Chen, F., Lin, X., Liu, Z., Zhang, H., Zhao, J., Li, K., Ye, Q., Li, Y., Lv, S., Yang, P., Wu, W., Li, Z., Lal, R., Tang, H., 2015. Potential benefits of climate change for crop productivity in China. Agric. For. Meteorol. 208, 76–84.
Ye, T., Nie, J., Wang, J., Shi, P., Wang, Z., 2015. Performance of detrending models of crop yield risk assessment: evaluation on real and hypothetical yield data. Stoch. Env. Res. Risk A. 29, 109–117.
Yue, Y., Li, J., Ye, X., Wang, Z., Zhu, A.X., Wang, J.A., 2015. An EPIC model-based vulnerability assessment of wheat subject to drought. Nat. Hazards 78, 1629–1652.
Zaitchik, B.F., Macalady, A.K., Bonneau, L.R., Smith, R.B., 2006. Europe's 2003 heat wave: a satellite view of impacts and land–atmosphere feedbacks. Int. J. Climatol. 26, 743–769.
Zeri, M., Cunha-Zeri, G., Gois, G., Lyra, G.B., Oliveira-Júnior, J.F., 2019. Exposure assessment of rainfall to interannual variability using the wavelet transform. Int. J. Climatol. 39, 568–578.
Zhao, J., Yang, X., Dai, S., Lv, S., Wang, J., 2015. Increased utilization of lengthening growing season and warming temperatures by adjusting sowing dates and cultivar selection for spring maize in Northeast China. Eur. J. Agron. 67, 12–19.